

## TIME TRANSFER USING WAAS: AN INITIAL ATTEMPT

Patrick Fenton  
NovAtel, Inc.  
1120 68th Ave. NE  
Calgary, Alberta T2E 8S5, Canada  
[pfenton@novatel.ca](mailto:pfenton@novatel.ca)

Bill Klepczynski  
Innovative Solutions International, Inc.  
1608 Spring Hill Road, Suite 200  
Vienna, VA 22182, USA  
[wklepczy@aol.com](mailto:wklepczy@aol.com)

Edward Powers  
U.S. Naval Observatory  
Time Service Department  
3450 Massachusetts Ave. NW  
Washington, DC 20392, USA  
[powers@drake.usno.navy.mil](mailto:powers@drake.usno.navy.mil)

Robert Douglas  
National Research Council  
Frequency and Time Standards  
Inst. for National Measurement Standards  
Ottawa, Ontario K1A 0R6, Canada  
[rob.douglas@nrc.ca](mailto:rob.douglas@nrc.ca)

### *Abstract*

*The FAA is currently developing the Wide Area Augmentation System (WAAS), a GPS Satellite-Based Augmentation System (SBAS) that will be used for navigation within the National Airspace System (NAS). WAAS consists of a multitude of ground reference stations and several geo-stationary communication satellites. The geo-stationary satellites will be broadcasting a "GPS"-like signal that can be used as a supplementary navigational signal and that will also contain GPS health status and correction data. The WAAS also offers a significant tool to the timing community.*

*There are several unique advantages of using the WAAS or any SBAS for frequency and time transfer:*

- 1. The geo-stationary satellites are always in view. They never set like the GPS and GLONASS satellites. This offers the ability for multiple sights to be permanently "phase-locked" together by locking themselves to the common WAAS signal.*
- 2. They do not have any intentional distortions like the GPS SA dither.*
- 3. WAAS system computes and broadcasts orbit and clock corrections for all GPS satellites in view thereby substantially removing the effects of SA on GPS.*
- 4. The geo-broadcast signals are cesium-based, generated and controlled by the WAAS network of cesium-based GPS receivers.*
- 5. The WAAS network computes a real-time observational ionospheric delay model for the coverage area. This model is broadcast over the WAAS signal so that an L1 single frequency user can make local corrections.*

*This paper describes an initial attempt at time transfer using the WAAS test transmissions currently broadcast from the INMARSAT Atlantic Ocean Region – West (AOR-W) satellite. The clocks being*

*compared are the master clock at USNO Washington and the master clock at NRC Ottawa. A 30-day data set is examined. It was obtained from dual frequency GPS/WAAS NovAtel receivers that were set up at both institutions. Comparisons are made between UTC(USNO), UTC(NRC), GPS time, and WAAS Network Time (WNT).*

## I. Introduction

A NovAtel WAAS Millennium Narrow Band Receiver was installed and operated at the United States Naval Observatory's (USNO). The receiver's oscillator was phase-locked to the USNO hydrogen maser master clock (MC2). The location of the temporary antenna installed on the roof was computed from 3 weeks of averaging of WAAS corrected GPS computed points. There were 107,420 points gathered. One point was collected every 15 seconds. The average computed position was:

N  $38^{\circ} 55' 13.8138''$ ,  
W  $77^{\circ} 03' 59.2032''$ ,  
Height 53.044 m (Ellipsoid)

The standard deviation of each point, Latitude, Longitude, and Height was 1.3 m, 1.2 m and 3.2 m respectively.

A second NovAtel Millennium receiver was installed at the Canadian National Research Council (NRC) in Ottawa. It was remotely operated from Calgary over the Internet with RapidRemote V1.5 software from QuarterDeck. This receiver was connected and phase-locked to NRC's hydrogen maser master clock (H4). The coordinates of NRC were also computed by taking a 3-week average. The average computed position was:

N  $45^{\circ} 27' 14.9814''$   
W  $75^{\circ} 37' 25.7839''$   
H 82.732m (Ell.)

The precise vector between NRC and USNO was computed by processing three separate 24-hour data sets using NovAtel's SoftServe Geodetic dual frequency postprocessing package. Holding NRC fixed at its WAAS averaged computed location, the phase vector position computed for USNO was:

N  $38^{\circ} 55' 13.7959''$   
W  $77^{\circ} 03' 59.1977''$   
H 51.784m (Ell.)

The vector distance between the two receivers was 759Km on a north-north-east baseline from USNO. The agreement between the three successive processing batches was better than 5cm. The difference between the 3-week averaged USNO point and the computed vector from NRC was 0.5m, 0.1m, 1.3m for Latitude, Longitude, and Height respectively. The vector-computed location for USNO was used for all processing because it was important to maintain a very accurate relative position between USNO and NRC for the very clock transfer computations.

## II. Data Collection

Data collection was commenced Oct 6 1999 and continued through to Nov 31 1999. Pseudo range and carrier phase measurements were made at 15-second intervals from GPS as well as the AOR-W WAAS GEO satellite. All of the broadcast data from the satellites was collected for subsequent postprocessing. Most of the analysis for this paper used 3 weeks of data from November 6 through to November 22. There were several data breaks and setup problems with the October data.

## III. Data Processing

The clock difference between any sight (say USNO) and GPS system time was computed by Equation (1):

$$GPSClockdiff_i(t) = Psr_i(t) + Tropc_i(t) + Ionoc_i(t) - RangeToSat_i(t) \quad (1)$$

Where:

$t$	is the time of measurement
$GPSClockdiff_i$	is the clock difference at time $t$ between the receiver's time and the GPS system time as measured by satellite $i$ .
$Psr_i$	is the measured pseudorange to satellite $i$
$Tropc_i$	is the Tropospheric correction for satellite $i$
$Ionoc_i$	is the Ionospheric correction for satellite $i$
$RangeToSat_i$	is the computed range to satellite $i$ using GPS broadcast ephemeris

$$GPSClockdiff(t) = \frac{1}{Nsats} \sum_{i=1}^{Nsats} GPSClockdiff_i(t) \quad (2)$$

Note that the receiver clock difference at any point in time can be further improved by averaging the computed clock differences from all satellites observed at that time using Equation (2). Typically there are around 8 satellites in view with a minimum of 4 and a maximum of 12. The NovAtel Millennium WAAS receiver was configured as 10 GPS L1+L2 plus 1 WAAS L1. This allowed for a maximum of 11 satellites tracked at any point in time.

To analyze the frequency stability of the Clockdiff measurement, the Allan deviation curve was computed using Equation (3).

$$AllanDeviation(T) = \sqrt{\frac{1}{2(N-1)} \sum_{i=T}^{NT} \left( \frac{Clockdiff_{i+T} - Clockdiff_i}{T} - \frac{Clockdiff_i - Clockdiff_{i-T}}{T} \right)^2} \quad (3)$$

Where:

T	is sample period (s)
N	is number of sample sets used in accumulation

To analyze the time stability of the Clockdiff measurement, a 2nd order low pass feed back filter

was used to "smooth" the data. The design of this "Smoother" filter was chosen to closely match a circuit that would slave a local GPS oscillator that was producing the *Clockdiff* measurement. Fig. 1 illustrates this filter.

The *Clockdiff* measurements are processed by passing the data repeatedly through the smoother filter with an adjustable time constant. The standard deviation of the smoothed data is computed for each time constant used. The low pass smoother characteristics indicate whether an improvement in timing accuracy can be made by averaging the instantaneous *Clockdiff* measurements with the use of a good local oscillator.

Frequency transfer function for Low pass Smoother second order loop is given by Equation (4):

$$H(\omega) = \frac{j2\zeta\omega_N\omega + \omega_N^2}{-\omega^2 + j2\zeta\omega_N\omega + \omega_N^2} \quad (4)$$

Where:

$$K_0 = \sqrt{2}\omega_N \quad \text{First Order Loop Gain} \quad (5)$$

$$K_1 = \omega_N^2 T \quad \text{Second Order Loop Gain} \quad (6)$$

$$\omega_N = \frac{8\mathcal{B}_L}{4\zeta^2 + 1} \quad \text{Loop Natural Frequency} \quad (7)$$

$$\zeta = \frac{\sqrt{2}}{2} \quad \text{Loop Damping Ratio} \quad (8)$$

$$T_c = \frac{1}{\zeta\omega_N} \quad \text{Loop Time Constant} \quad (9)$$

$$\mathcal{B}_L = \frac{3}{4T_c} \quad \text{Loop Noise Bandwidth Hz} \quad (10)$$

The clock difference between any receiver and WAAS Network Time (WNT) was computed by Equations (11) and (12):

$$WNTClockdiff_i = Psr_i + Tropc_i + Ionoc_i + WAASFast_i + WAASSlow_i - RangeToSat_i \quad (11)$$

$$WNTClockdiff(t) = \frac{1}{Nsats} \sum_{i=1}^{Nsats} WNTClockdiff_i(t) \quad (12)$$

Where:

$WNTClockdiff_i$  is the clock difference between the receiver's time and the WNT as measured by satellite  $i$ .

$WAASFast_i$  is the fast clock correction for satellite  $i$

$WAASSlow_i$  is the slow orbital error and slow clock correction for satellite  $i$

The  $WNTClockdiff$  was analyzed by computing its Allan deviation and smoother characteristics by Equations (3) and (4).

The clock difference between two sights on the ground (say USNO and NRC) can be computed using either Equation (13) or (14).

$$DClockdiff_i = GPSClockdiff_i^{USNO} - GPSClockdiff_i^{NRC} \quad (13)$$

$$DClockdiff_i = WNTClockdiff_i^{USNO} - WNTClockdiff_i^{NRC} \quad (14)$$

Where  $DClockdiff_i$  is the clock difference between the USNO and NRC clocks as measured by satellite  $i$ .

It would be expected that the  $DClockdiff$  computed from Equation (14) using the improved WAAS orbit data would significantly improve the results as compared with only the broadcast GPS positions as computed by Equation (13). Equation (14) was used for the results of this paper.

The correction for the ionosphere ( $Ionoc_i$ ) was computed from the difference between GPS smoothed L1 and L2 pseudorange measurements. Fig. 2 illustrates the ionospheric correction filtering for a single GPS L1-L2 satellite pass. The differenced pseudorange is smoothed by the differenced carrier phase measurement. Essentially, the differenced carrier phase values are used for the ionosphere after they are adjusted to the average offset that maps it onto the differenced pseudorange curve.

The pseudorange value, corrected for ionospheric delay, was similarly represented by the L1 Carrier measurement, corrected for ionospheric delay. The carrier provided a low noise estimate of the pseudorange value. Fig. 3 illustrates this process. Fig. 3 shows the misclosure between the carrier phase and the pseudorange value. Note that the carrier phase fits the pseudorange measurements with zero mean and 0.1 ns standard deviation over this 6-hour pass. Most of the excursions between the code and carrier are caused by multipath interference on the pseudorange measurement at the receiving antenna.

Only GPS measurements from satellite passes that were longer than 3 hours where the satellite was 20 degrees above the horizon were used in the calculations. Having a high elevation cut-off angle removed most of the effects of multipath interference in the data. Having long sets of satellite data enabled very accurate carrier fit estimates for the ionospheric correction and the L1 pseudorange smoother.

A standard Hopfield model was used for the tropospheric correction.

## IV. Discussion of Results

The difference between USNO and GPS system time was computed and is illustrated in Fig. 4. This difference was included as a common denominator benchmark process. Most GPS timing receivers today use this observable to provide time reference information. Note that the 43ns standard deviation caused by the DOD's selective availability (SA) (intentional dither) is very slow in nature and must be smoothed over a very long time constant in order to be removed. The "Smoothen" curve in Fig. 5 illustrates the correlation characteristic of this process. Note, in Fig. 5 the smoothing time constant must be at least 55,000 seconds before a significant filtering of the SA is accomplished and has been reduced to less than 10ns. Note also that the Allan deviation is dominated by SA starting out at  $4 \times 10^{-10}$  at a 30-second measurement interval and falls at a constant 10dB per decade, showing that the frequency dither of SA is uncorrelated.

Fig. 6 represents a 3-week history of the difference between the clock at USNO and WNT. The standard deviation of the clock difference during this period was 11 ns. But there was significant low frequency noise presumably caused by clock steering oscillations in the WAAS system control segment. We make this assumption because the oscillations occur on even 12-hour boundaries (coincident with the WAAS steering algorithm). Fig. 7 shows the difference between the USNO clock and WNT during the later 12 hours of November 14th. Note that the fit between USNO and WNT over short 12-hour segments is in the nanosecond noise level. This result is very significant in that once the WAAS control segment smooths out its clock steering oscillations, the long-term clock errors will be at the nanosecond level.

Fig. 8 shows the Allan deviation and smoothing characteristics of the 3-week USNO-WNT data set. Note, in Fig. 8, that the Allan deviation flattens out to  $3 \times 10^{-13}$  at 10,000 seconds because of the network steering oscillations. Similarly, the smoother time constant does not significantly filter the oscillations until its time constant is over 2 days in length.

Fig. 9 shows the differential time drift between USNO and the NRC master clock. We used the WAAS corrected orbit Equation (14) to produce these results. The standard deviation from a linear fit (of 8ns/day) was less than 1ns!

Using the GPS broadcast orbits increase the standard deviation of the clock difference by a factor of 2, (an increase from 0.6 to 1.2 ns).

Fig. 10 shows the Allan deviation and smoothing characteristics of the WAAS orbit differential timing data. It shows that the smoother does not converge until the time constant gets longer than the longest satellite pass tracking time (~10,000s). This is caused by the correlation of the phase smoothing process of the ionosphere and the L1 Pseudorange. Note that the standard deviation of the Smoothed clock offset drops below 400ps after 1 day of smoothing.

The Allan variance of the differential data starts off at  $6 \times 10^{-13}$  at 120-second sample period and reduces linearly down to  $3 \times 10^{-15}$  at 2.5-Day sample period (200,000s).

## V. Conclusions

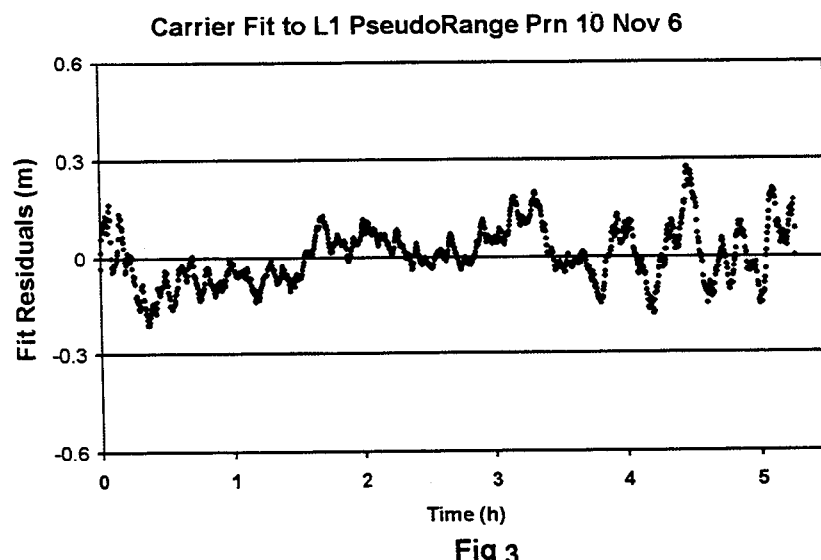
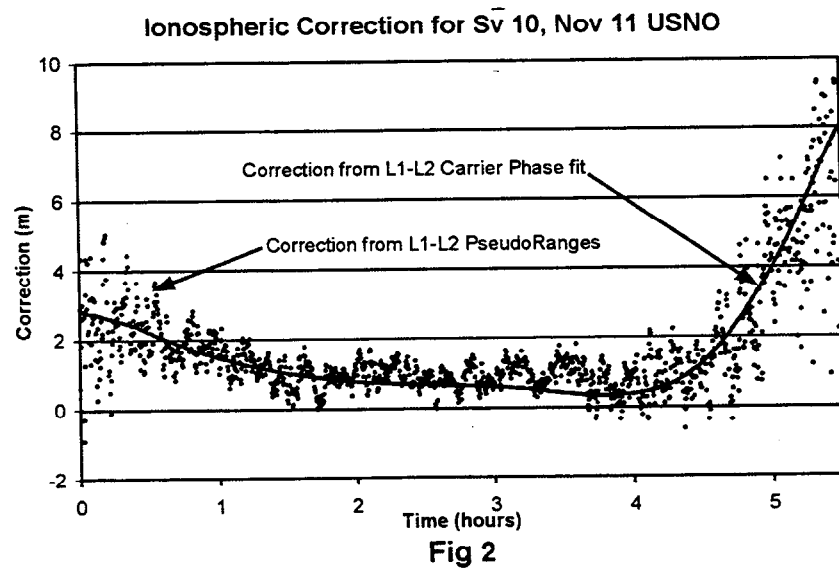
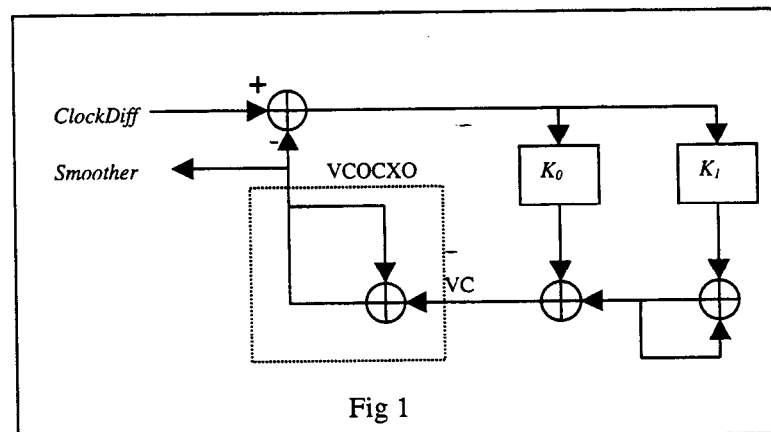
The receiver was able to track WNT with a noise level of 1.5ns. Using the WAAS computed orbits provided the common view multiple satellite time transfer of less than 1ns (measured 0.7ns). This method of providing time transfer is simple and effective. The biggest sources of error were the transitions between satellites (constellation switches).

These results, at this early stage in the development of the WAAS, indicate the future promise of this technique for time transfer and time distribution.

## References

J. L. LaMance, A. Brown, B. Haines, W. Bertiger and S. Wu, *Time Calibration Using the INMARSAT geostationary Overlay Signal From the AOR-W Satellite*, Proc. of ION-GPS 95.

T. E. Melgard, D. Last and B. Thomas, *Precise GPS Time Transfer to a Moving Vehicle*, Proc. of ION-GPS 95.



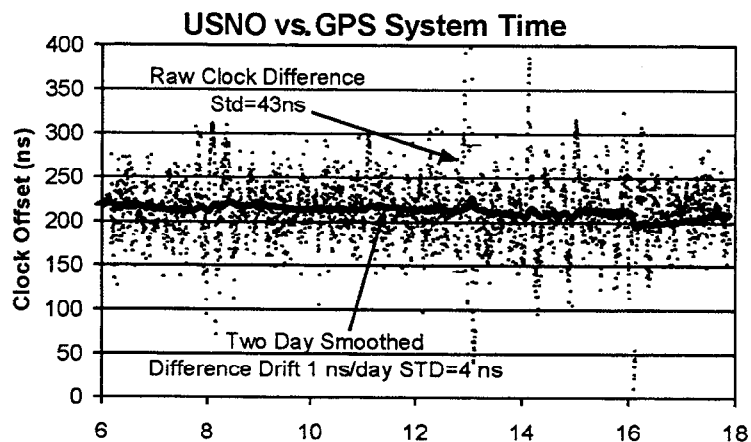


Fig 4

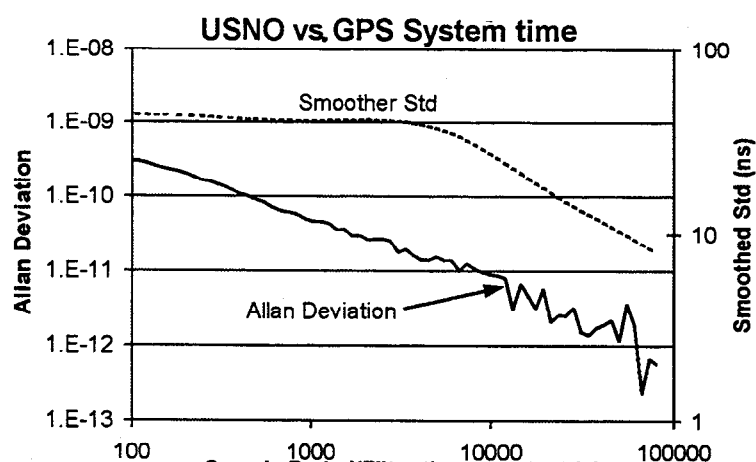


Fig 5

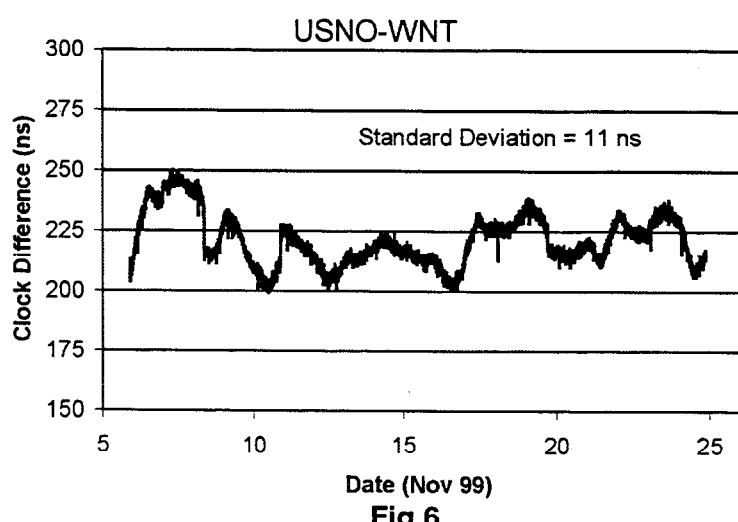
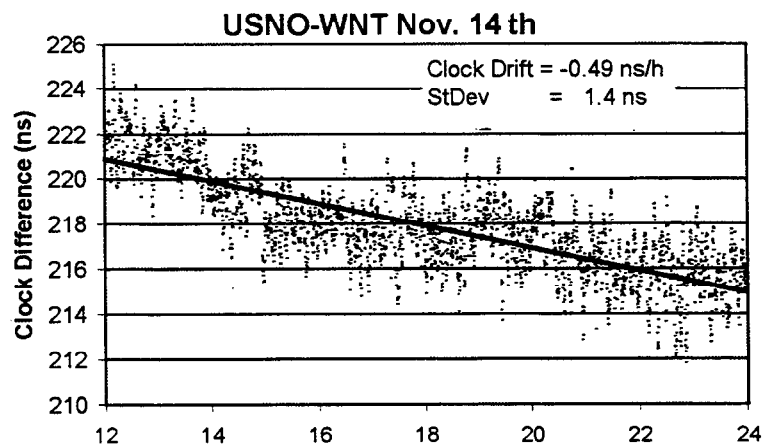
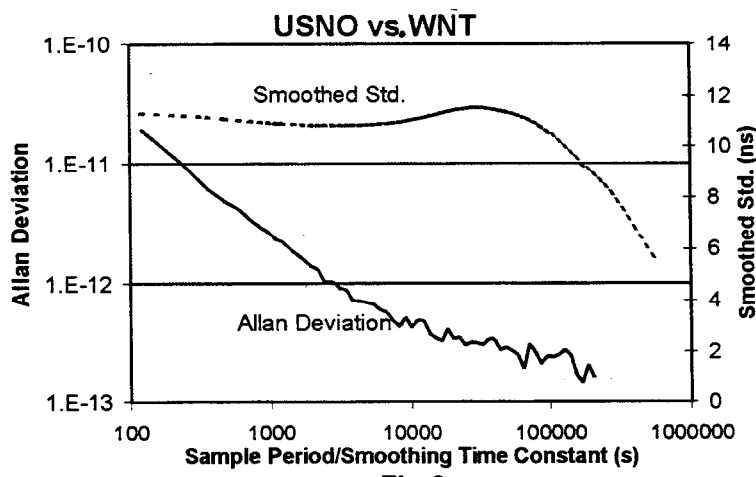


Fig 6



**Fig 7**



**Fig 8**

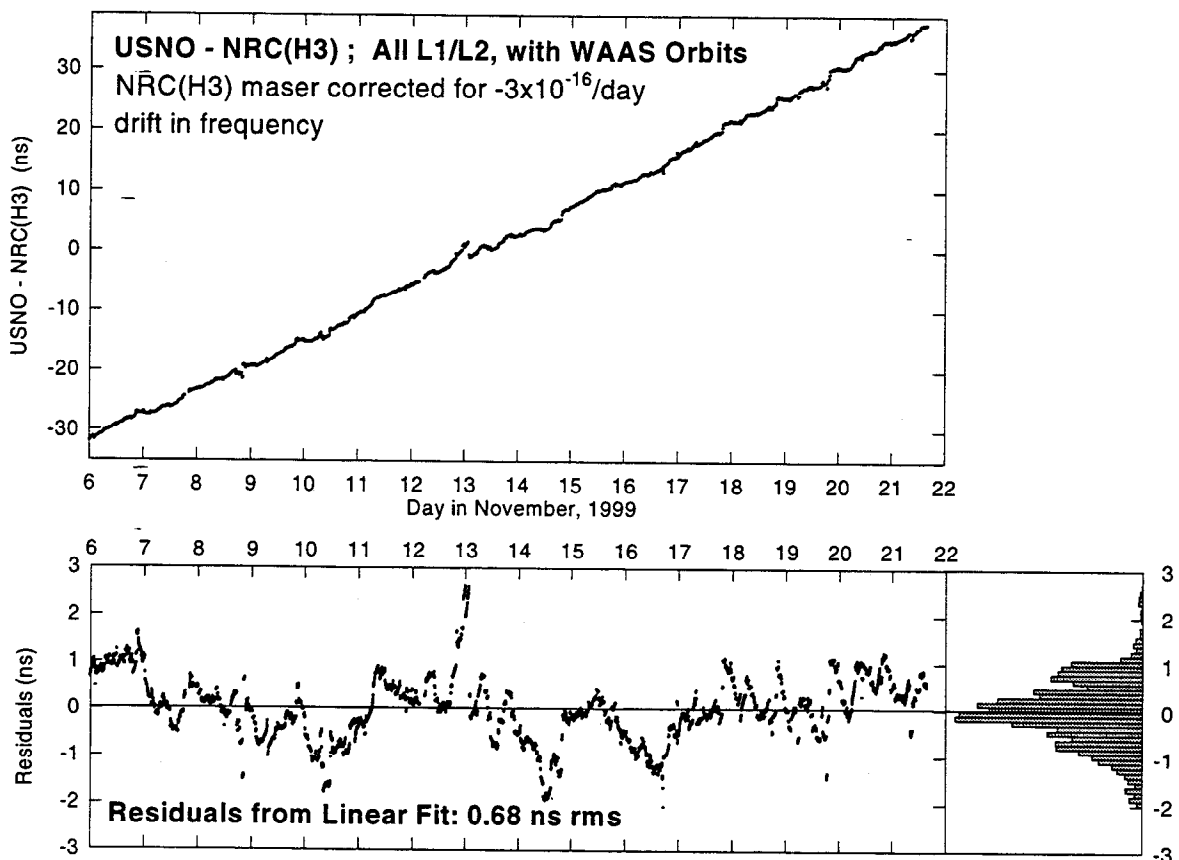


Fig 9

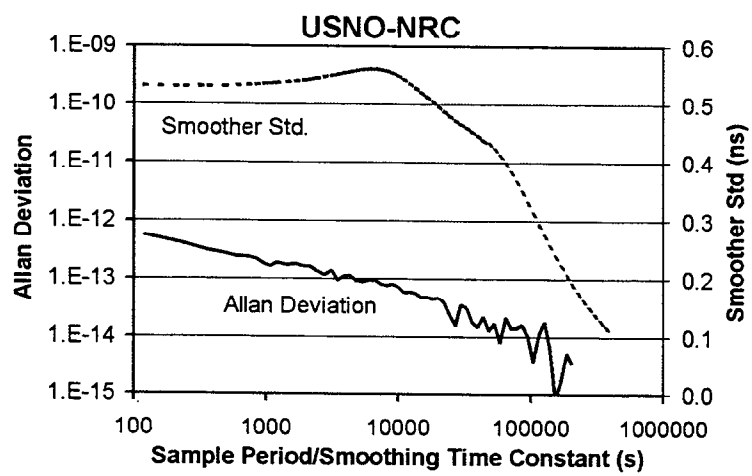


Fig 10

## Questions and Answers

HUGO FRUEHAUF (Odetics): How does the fact that the GUS is, of course, stationary and the satellite is sort of making a figure-eight ground trace — is there a correlation in the timing data that you see from that figure eight?

PATRICK-FENTON (NovAtel): Well, the figure eight is plotting a very slow multi-path that we see in the diagram. The multi-path, instead of in a typical GPS multi-path, is in the order of 3 to 5 minutes, where the GUS multi-path is like 5 to 6 hours. So you can see that errors correlated to the little figure eight. But as far as using the geostationary satellites, it's really nice because it's not moving and you can put a dish on it and get around that kind of stuff.